

Investigation on Ni₃Al-Ni₇Hf₂ unidirectionally solidified eutectic composite

S. W. MA, Y. R. ZHENG, Z. C. RUAN

Beijing Institute of Aeronautical Materials, Beijing, 100095

E-mail: biamqbjs@public3.bts.net.cn

The formation of a Ni₃Al(γ')+Ni₇Hf₂ unidirectionally solidified lamellar eutectic composite has been investigated in this paper. The results show that Ni-5.8Al-32Hf alloy, which has the Ni₃Al+Ni₇Hf₂ eutectic structure, is a suitable composition of D.S eutectic material. The melting range of this composition is 41 °C as determined by DTA. The critical ratio of G/R for Ni₃Al+Ni₇Hf₂ eutectic is found to be $5 \times 10^5 \text{ }^\circ\text{C} \cdot \text{s} \cdot \text{cm}^{-2}$, and the lamellar Ni₃Al+Ni₇Hf₂ eutectic aligned parallel to the direction of solidification was made with $R = 5 \text{ } \mu\text{m/s}$ and $G = 250 \text{ }^\circ\text{C/cm}$. The investigation shows that the lamellar eutectic has a preferred crystallographic orientation between the Ni₃Al and Ni₇Hf₂ lamellae, i.e., $(111)_{\text{Ni}_3\text{Al}} // (100)_{\text{Ni}_7\text{Hf}_2}$ and $[110]_{\text{Ni}_3\text{Al}} // [010]_{\text{Ni}_7\text{Hf}_2}$. The lamellar Ni₇Hf₂ did not degrade or coarsen obviously, and no harmful phase formed in the interface of Ni₃Al/Ni₇Hf₂ after long time soaking of 1100 °C/110 h. This demonstrates that the Ni₃Al+Ni₇Hf₂ lamellar eutectic has high interface thermal stability. © 1999 Kluwer Academic Publishers

1. Introduction

In recent years, it is paid attention to the directionally solidified (D.S) eutectic superalloys (*in situ*-composition materials), which have higher strength than D.S nickel base superalloys at high temperature [1]. In order to develop this kind of material further, many eutectic systems have been studied [2, 3].

As a matrix for a structural composite formed by eutectic solidification, the intermetallic compound Ni₃Al is the most interesting. The importance of Ni₃Al is well recognized in nickel-base superalloys [4, 5] which are strengthened by precipitates of γ' . It may be strengthened by other elements in solid solution [6]. As a single crystal, Ni₃Al exhibits extensive ductility at room temperature [7].

Since Ni₃Al was recognized as an ideal matrix for high melting eutectics, systems between Ni₃Al and a second intermetallic were sought to develop a D.S eutectic material with higher thermal stability and better transverse-plasticity. The preliminary results showed that microhardness of Ni₇Hf₂ phase was equivalent to that of Ni₃Al and a eutectic of $\gamma' + \text{Ni}_7\text{Hf}_2$ did not crack by cold rolling. Besides, the diffusion ability of Hf in Ni₃Al phase was very low even at high temperature [8]. Therefore, directionally solidified Ni₃Al-Ni₇Hf₂ eutectic composite was investigated in detail in this paper, including the microstructure, solidification behavior, crystallography relationship and thermal stability of the eutectic composite material.

2. Experimental

The composition of the alloy was determined to be Ni-5.8Al-32Hf (wt %) based on the isothermal-section of Ni-Al-Hf system at 1200 °C [9].

The alloy was prepared as a 150 g ingot by nonconsumable electrode arc melting in 3×10^4 Pa pressure argon. The ingot was remelted three times to improve the compositional homogeneity. The weight variation of the ingot during melting was small and the nominal composition of the alloy was taken as the actual composition.

The metallographic specimens were etched in a mixing solution of 10% hydrogen fluoride, 20% nitric and 70% water. Thin foil for TEM was prepared by twin-jet thinning in a solution of 59% methanol +35% butanol +6% perchloric acid at -25 °C, and examined by H800 electron microscope operating at 200 KV.

The phase transition temperature and the melting range were determined by DTA at a cooling rate of 10 °C/min under the protection of argon. The unidirectional solidification was carried out in a high temperature gradient D.S furnace using Ga-In-Sn liquid metal cooling.

3. Results and discussion

3.1. Microstructure of as cast alloy

Fig. 1 shows the typical microstructure of the as cast alloy. Two types of eutectic zones (A and B) and minor primary phase Ni₇Hf₂ exist in the alloy. Further analysis reveals that region A is Ni₃Al+Ni₇Hf₂ eutectic, and the white region B is fine eutectic structure consisting of NiAl and Ni₇Hf₂ phases.

Fig. 2 is the quenched microstructure of alloy near the solid-liquid zone during the unidirectional solidification. It shows that NiAl+Ni₇Hf₂ eutectic forms in the intereutectic of Ni₃Al+Ni₇Hf₂ during the later solidification due to non-equilibrium solidification. The

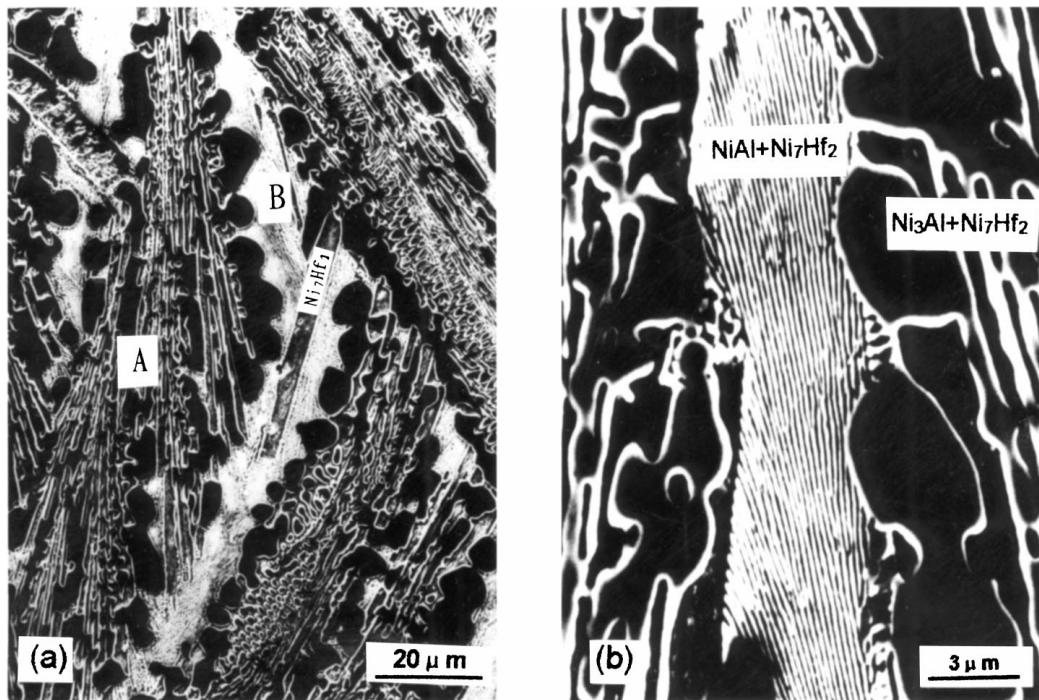


Figure 1 The microstructure of Ni-5.8Al-32Hf (wt %) alloy as cast . (a) The typical morphology; (b) NiAl+Ni₇Hf₂ eutectic existed in region B shown in Fig. 1a.

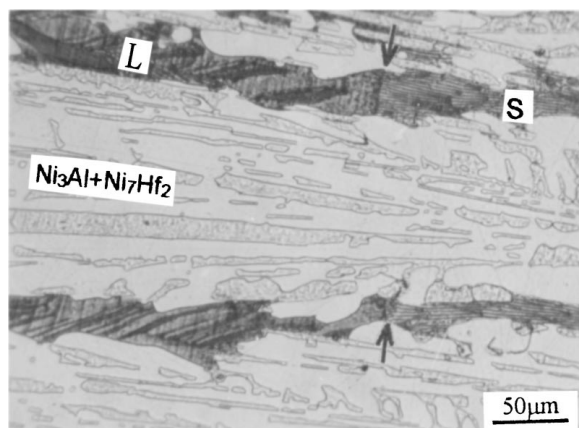


Figure 2 The solidification interface of lower melting region existed in the interdendrite.

formation of NiAl+Ni₇Hf₂ at high solidification rate implies the existence of a ternary invariant reaction: L+Ni₃Al \rightarrow NiAl+Ni₇Hf₂. It also indicates a saddle point on the L \rightarrow Ni₃Al+Ni₇Hf₂ liquidus valley. On the basis of these analyses, a schematic liquidus projection in this region is shown in Fig. 3.

Three peaks in the DTA curve of the alloy (Fig. 4) represent different phase transformations during the solidification process, i.e., the precipitation of primary phase Ni₇Hf₂ in 1225–1232 °C, reaction of L \rightarrow Ni₃Al+Ni₇Hf₂ in 1210–1212 °C, and L+Ni₃Al \rightarrow NiAl+Ni₇Hf₂ in the 1191–1210 °C. The alloy melting range $\Delta T = 41$ °C was also obtained from the DTA curve.

3.2. Unidirectional solidification of the alloy

Fig. 5 shows the microstructures of unidirectionally solidified alloys with different solidification rate (R) un-

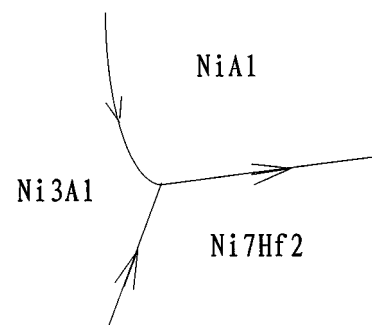


Figure 3 Liquidus projection for the region of interest in the Ni-Al-Hf system.

der the same temperature gradient (G). Region A and B still exist in unidirectionally solidified alloys. Region A is the eutectic of Ni₃Al+Ni₇Hf₂ and region B is the NiAl+Ni₇Hf₂ eutectic. Electron probe analysis shows that the composition of region B is about Ni-7.5Al-32.5Hf (wt %). The existence of NiAl impairs the high temperature strength of alloys. Therefore NiAl should be avoided. Fortunately, this phase can be eliminated by control of the D.S solidification conditions.

Two obvious changes have taken place with the decrease of solidification rate (R) from 20 to 5 $\mu\text{m/s}$. One is the decrease of segregation degree, indicated by the volume fraction of NiAl+Ni₇Hf₂ eutectic. The other is the morphology of Ni₃Al+Ni₇Hf₂ eutectic. As the rate of growth decreases, the ratio of G/R becomes greater and the solidification process tends to be steady plane-front growth, the morphology of Ni₃Al+Ni₇Hf₂ eutectic changes from flower form to discontinuous lamellae, and then to a continuous lamellar structure (as shown in Fig. 5a to d). D.S tests reveal that solidification rate $R = 5$ $\mu\text{m/s}$ is a critical value with the temperature gradient $G = 250$ °C/cm. (i.e. critical ratio

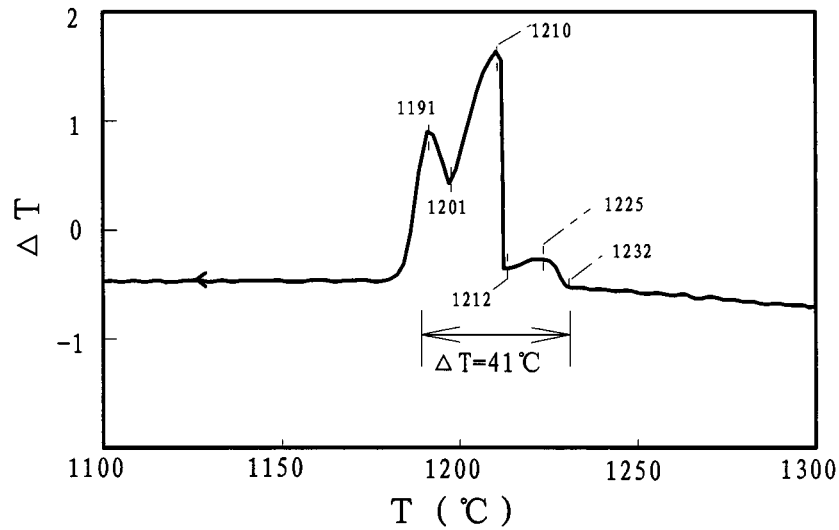


Figure 4 DTA curve of Ni-5.8Al-32Hf (wt %) alloy at a cooling rate of $10^{\circ}\text{C}/\text{min}$.

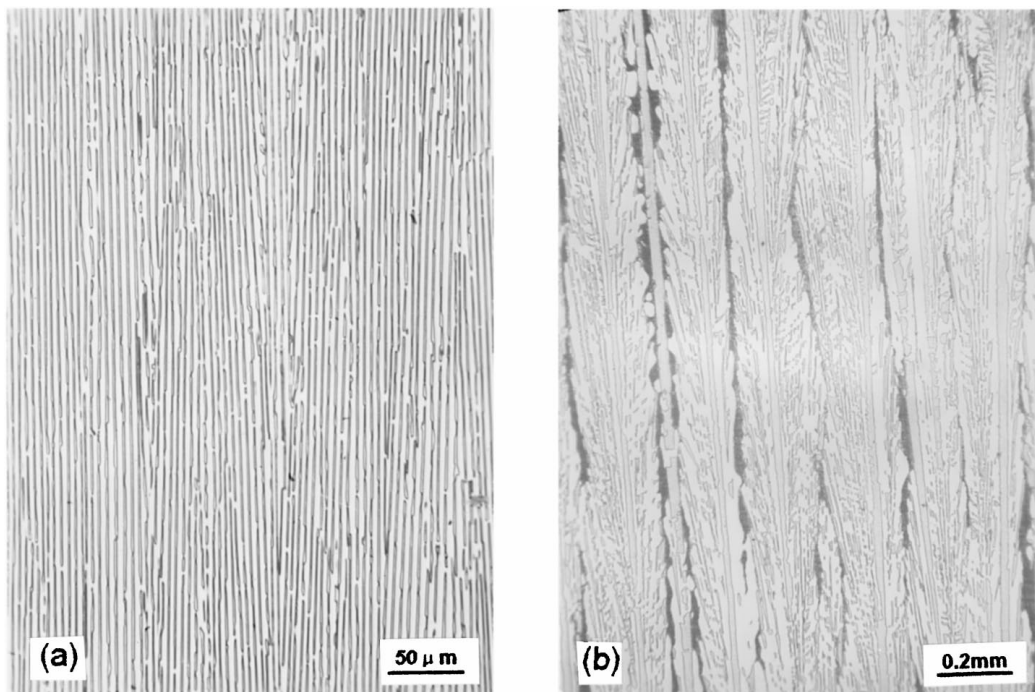


Figure 5 Longitudinal microstructures of Ni-5.8Al-32Hf (wt %) alloy with different solidification rate (R) under Gradient (G) $250^{\circ}\text{C}/\text{cm}$. (a) $R = 5 \mu\text{m}/\text{s}$; (b) $R = 6 \mu\text{m}/\text{s}$; (c) $R = 10 \mu\text{m}/\text{s}$; (d) $R = 20 \mu\text{m}/\text{s}$. (Continued)

of $G/R = 5 \times 10^5 \text{ }^{\circ}\text{C} \cdot \text{s} \cdot \text{cm}^{-2}$). Under the critical G/R , the $\text{Ni}_3\text{Al}+\text{Ni}_7\text{Hf}_2$ lamellar aligned parallel to the direction of solidification, and the $\text{NiAl}+\text{Ni}_7\text{Hf}_2$ eutectic was suppressed completely.

3.3. Crystallography relationship

Ni_7Hf_2 has the monoclinic structure with $a = 1.2102 \text{ nm}$, $b = 0.8191 \text{ nm}$, $c = 0.4657 \text{ nm}$ and $\beta = 95.50^{\circ}$. The (100) plane is close packed [9]. Fine internal striations parallel to the growth direction within Ni_7Hf_2 were observed (Fig. 6a), which corresponded to twinning on the (100) basal plane.

A preferred crystallography relationship was found between the Ni_3Al and Ni_7Hf_2 lamellar, i.e., $(111)_{\text{Ni}_3\text{Al}}// (100)_{\text{Ni}_7\text{Hf}_2}$ and $[110]_{\text{Ni}_3\text{Al}}//[010]_{\text{Ni}_7\text{Hf}_2}$. The interfacial plane was composed of two densely packed planes of

phases (Ni_7Hf_2 , Ni_3Al), which mean the interface is in low energy state. An electron micrograph and corresponding electron diffraction pattern which exhibit this relationship are shown in Fig. 7.

3.4. Interface thermal stability of $\text{Ni}_3\text{Al}+\text{Ni}_7\text{Hf}_2$ eutectic

Fig. 8 shows the transverse microstructure of D.S. $\text{Ni}_3\text{Al}+\text{Ni}_7\text{Hf}_2$ eutectic materials after long time soaking of $1100^{\circ}\text{C}/110 \text{ h}$ (93% melting point) compared with unheated microstructure. The lamellar Ni_7Hf_2 did not degrade or coarsen obviously, and no harmful phase formed in the interface of $\text{Ni}_3\text{Al}/\text{Ni}_7\text{Hf}_2$. The investigation shows the $\text{Ni}_3\text{Al}+\text{Ni}_7\text{Hf}_2$ lamellar eutectic has high interface thermal stability, which is mainly due to the low diffusion ability of Hf in γ' at high

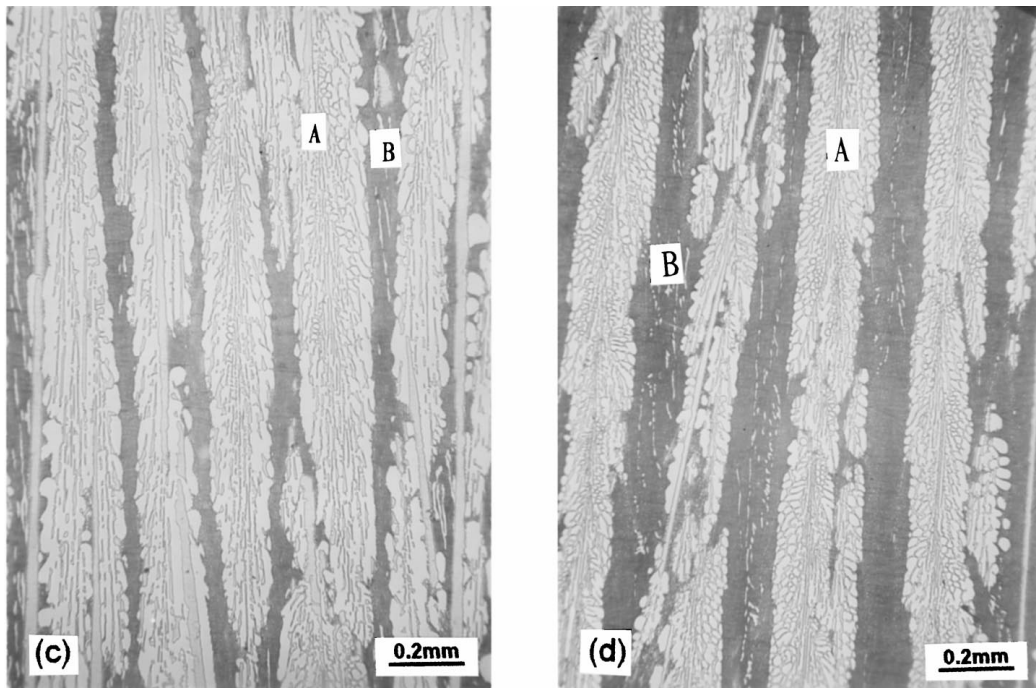


Figure 5 (Continued).

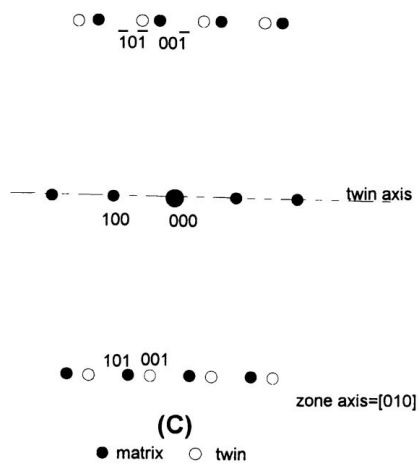
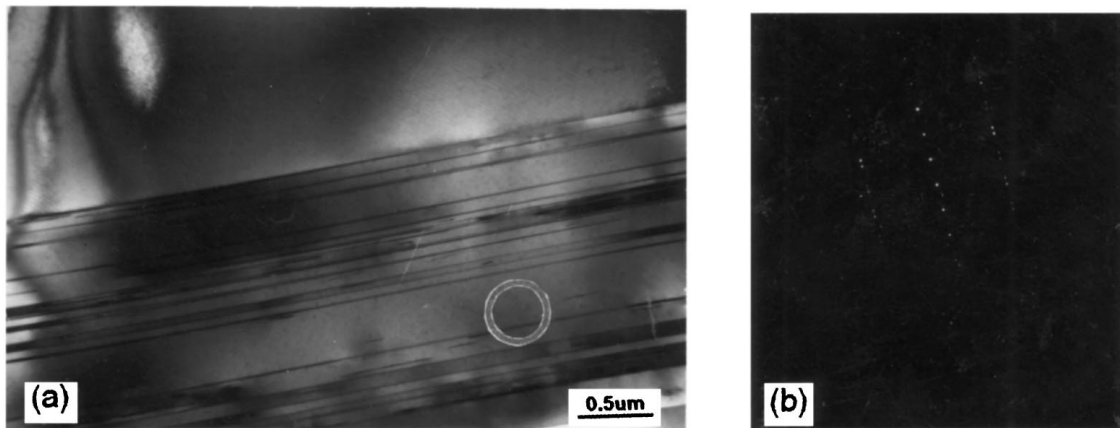


Figure 6 The Ni_7Hf_2 phase in D.S $Ni_3Al+Ni_7Hf_2$ eutectic at $G = 250^\circ C$, $R = 5 \mu m/s$. (a) twinning within the Ni_7Hf_2 phase; (b) Selected area diffraction pattern; (c) Indexing of diffraction pattern.

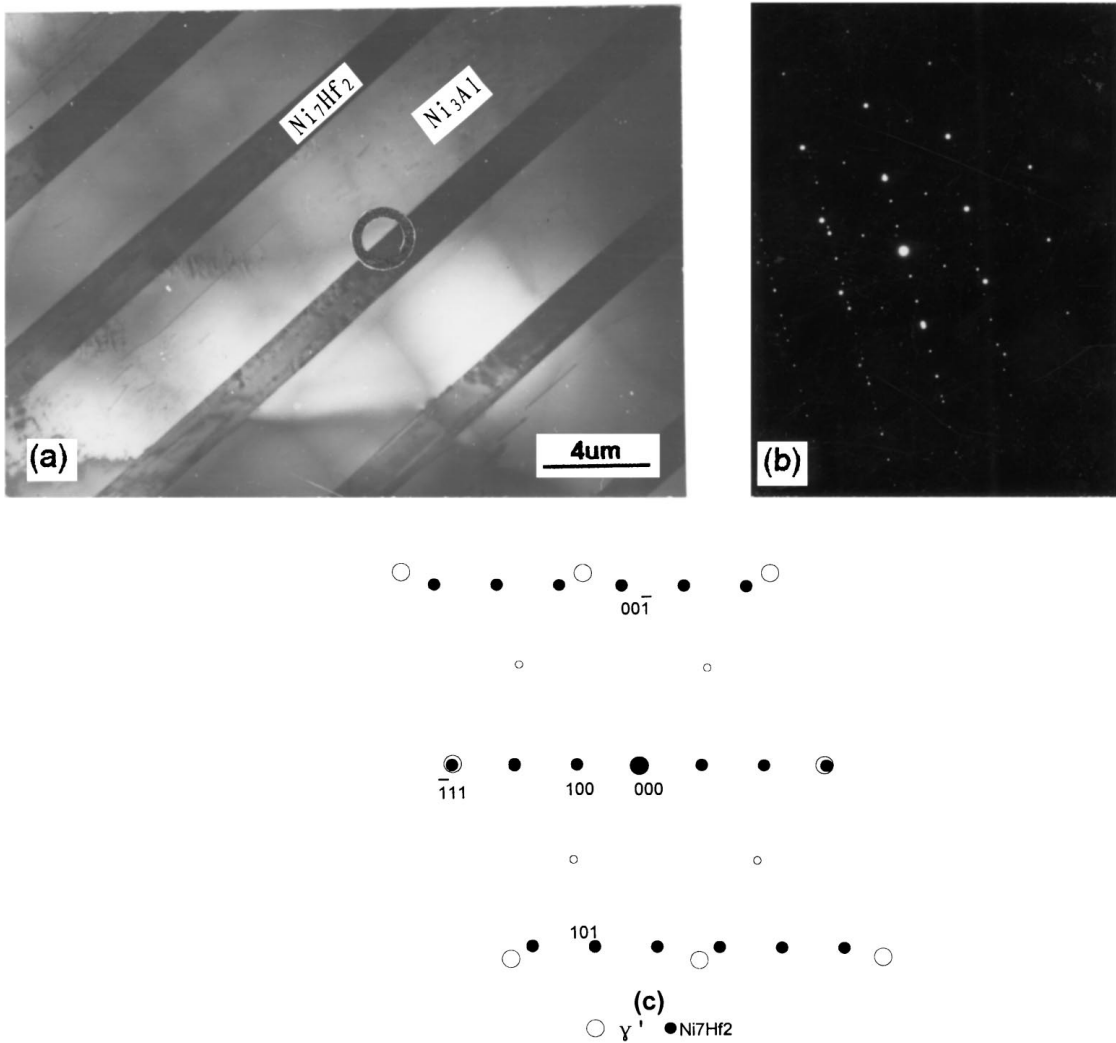


Figure 7 Transmission Electron Micrograph and Diffraction Pattern of D.S $\text{Ni}_3\text{Al-Ni}_7\text{Hf}_2$ lamellar eutectic. (a) Bright field of $\text{Ni}_3\text{Al-Ni}_7\text{Hf}_2$ lamellar eutectic; (b) selected area diffraction, zone Axis of Ni_3Al , $[110]$. Zone Axis of Ni_7Hf_2 , $[010]$; (c) Indexing of diffraction pattern.

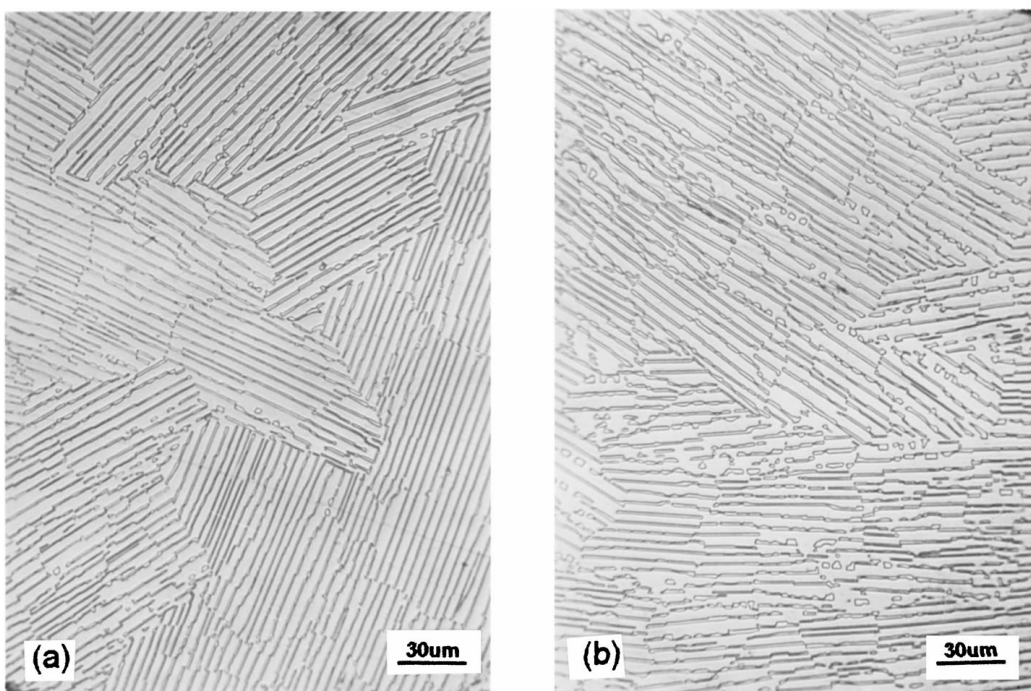


Figure 8 Comparison of microstructure of D.S $\text{Ni}_3\text{Al+Ni}_7\text{Hf}_2$ eutectic (a) unheated alloy; (b) heated by $1100^\circ\text{C}/110\text{ h}$.

temperature [8] and low energy of the interface due to the preferred crystallography relationship of the two phases.

4. Conclusions

1. Ni-5.8Al-32Hf is a proper composition for D.S eutectic, and consist of eutectic $\text{Ni}_3\text{Al}+\text{Ni}_7\text{Hf}_2$ mainly. Some NiAl exists in as-cast alloys, but can be eliminated by control of DS processing.

2. Ni-5.8Al-32Hf alloy has a melting range 41°C ($1191\text{--}1232^\circ\text{C}$) and the critical G/R ratio of $5 \times 10^5 \text{ }^\circ\text{C} \cdot \text{S} \cdot \text{cm}^{-2}$. Under the critical G/R , the lamellar $\text{Ni}_3\text{Al}+\text{Ni}_7\text{Hf}_2$ is aligned parallel to the direction of solidification.

3. The lamellar $\text{Ni}_3\text{Al}+\text{Ni}_7\text{Hf}_2$ eutectic has the following orientation relationships: $(111)_{\text{Ni}_3\text{Al}}// (100)_{\text{Ni}_7\text{Hf}_2}$ and $[110]_{\text{Ni}_3\text{Al}}// [010]_{\text{Ni}_7\text{Hf}_2}$, and high interface thermal stability was found.

Acknowledgement

This work was supported by National Natural Science Foundation of CHINA. The number of contract is 59471009.

References

1. R. G. MENZIES, In Superalloy 1988, Six International Symposium on Superalloys, Pennsylvania, 1988, edited by D. N. Duhl *et al.* (The Metallurgical Society, Pennsylvania, 1988) p. 355.
2. H. BIBRING, T. KHAN, M. RABINOVITH and J. STOHR, In Superalloys Metallurgy and Manufacture, Third International Symposium, Pennsylvania September 1976, edited by B. H. Kear (Claiter's Publishing Division, Louisiana, 1976) p. 331.
3. M. R. JACKSON and J. L. WALTER, In Superalloys Metallurgy and Manufacture, Third International Symposium, Pennsylvania September, 1976, edited by B. H. Kear (Claiter's Publishing Division, Louisiana, 1976) p. 341.
4. R. D. RAWLINGS and A. E. STATON, *J. Mater. Sci.* **3** (1975) 505.
5. A. BALL and R. E. SMALLMAN, *Acta Metall.* **11** (1966) 1517.
6. R. W. GUARD and J. H. WESTBROOK, *Trans. AIME.* **215** (1959) 807.
7. S. M. COPLEY and B. H. KEAR, *ibid.* **239** (1967) 977.
8. S. W. MA and Y. R. ZHENG, *Chinese Journal of Materials Research* **2** (1996) 149.
9. P. NASH and D. R. F. WEST, *Metal Science* **8** (1981) 347.

*Received 23 December 1997
and accepted 16 April 1999*